

# Anomalous properties of the band-edge states in large two-dimensional photonic quasicrystals

Yun Lai,<sup>1</sup> Zhao-Qing Zhang,<sup>1</sup> Chi-Hou Chan,<sup>2</sup> and Leung Tsang<sup>2</sup>

<sup>1</sup>*Department of Physics, Hong Kong University of Science and Technology, Clear Water Bay, Kowloon, Hong Kong*

<sup>2</sup>*Department of Electronic Engineering, City University of Hong Kong, Kowloon, Hong Kong*

(Received 15 May 2007; published 29 October 2007)

By using the sparse-matrix canonical-grid method, we performed large-scale multiple-scattering calculations to study band-edge states in large-sized two-dimensional photonic quasicrystals. We find that the band-edge states evolve in an abrupt and irregular way when the sample size is increased. New states with reduced symmetries can emerge at the band edge in large samples. Strong multifractal behaviors in the wave functions are also observed. Our findings unveil important differences between quasiperiodic and periodic systems at band edges.

DOI: [10.1103/PhysRevB.76.165132](https://doi.org/10.1103/PhysRevB.76.165132)

PACS number(s): 42.70.Qs, 41.20.Jb, 61.44.Br

## I. INTRODUCTION

The propagation of classical waves in quasiperiodic structures has attracted an increasing amount of attention in recent years.<sup>1–23</sup> Quasiperiodic composites, such as photonic quasicrystals, can offer more flexibility in designing the properties of electromagnetic waves than their periodic counterparts. In one dimension, the states in quasiperiodic multilayers and the evolution of spectrum with sample size have been extensively studied.<sup>1–4</sup> Many interesting phenomena such as critical states and singular continuous spectrum have been discovered.<sup>1,2</sup> In two dimensions, recently, it has been shown that large full band gaps can be opened in photonic quasicrystals with small dielectric contrast due to the high rotational symmetry of a quasiperiodic structure.<sup>5–8</sup> Various wave phenomena that depend on the existence of band gaps, such as defects and waveguides, have also been extensively studied.<sup>11–15</sup>

Recently, a wide interest has been attracted to the band-edge states in quasiperiodic composites.<sup>4,16–23</sup> Firstly, the property of wave functions at band edges in quasiperiodic structures remains an interesting and unresolved topic.<sup>24</sup> By observing the liquid surface wave on a quasiperiodically drilled bottom, the wave function at the band edge is shown to be a plane wave with quasiperiodic modulation.<sup>16</sup> Strongly suppressed group velocity has also been observed at the band-edge states of Fibonacci photonic quasicrystals by ultrashort pulse interferometry.<sup>4</sup> Secondly, great achievements have been made in the applications of the band-edge states in photonic crystals.<sup>25–29</sup> However, recent studies showed that the band-edge states in photonic quasicrystals can support various applications with novel and promising properties that are unrealizable by using the band-edge states in photonic crystals.<sup>17–21</sup> For example, lasing action of tenfold rotational symmetry at the band-edge states has been observed in photonic quasicrystals with a Penrose lattice.<sup>17</sup> Higher-order harmonic generations with more flexibility,<sup>18–20</sup> even simultaneous phase matching of arbitrary optical frequency-conversion processes,<sup>21</sup> have been investigated in nonlinear photonic quasicrystals.

However, previous studies on the band-edge states in quasiperiodic composites, especially in two dimensions, were conducted in a limited number of samples.<sup>16,17</sup> Thus, how the

properties of the band-edge states evolve with sample size were not studied, and the effects due to the quasiperiodic long-range order were not fully manifested in these studies. In order to fully explore these effects, large-sized samples are required. Theoretically, the bottleneck of this problem lies in the difficulty in computing large-sized multiple-scattering systems. The Born approximation which is valid for small systems may become invalid.<sup>17,22</sup>

In this work, we study the properties of the band-edge states for electromagnetic waves in large-sized two-dimensional photonic quasicrystals by using the multiple-scattering theory (MST) in conjunction with the sparse-matrix canonical-grid (SMCG) method.<sup>30</sup> On the one hand, the SMCG method allows us to do large-scale calculations efficiently so that the quasiperiodic long-range order effects can be studied, as in the study of acoustic waves in large-sized phononic quasicrystals;<sup>23</sup> on the other hand, the MST method allows us to calculate the wave functions of the band-edge states. These wave functions are not only academically interesting, but also important in applications of lasing and nonlinear optical effects in photonic quasicrystals. As a result, we have observed an abrupt and irregular evolution of the band-edge state with increased sample size. The wave functions exhibit repeated local resonances, which are induced by repeated clusters in the quasiperiodic structure. New states with reduced symmetries, which are absent in smaller samples, can emerge at the band edge in a sufficiently large sample. These findings show the important differences between quasiperiodic and periodic systems at band edges.

## II. SYSTEM AND NUMERICAL METHODS

We consider a photonic quasicrystal consisting of a 12-fold symmetric quasiperiodic lattice of dielectric cylinders placed in air. The 12-fold quasiperiodic lattice is composed by the vertices of a square-triangle tiling, which is generated from a dodecagonal seed structure by using the Stamfli inflation rule.<sup>7</sup> In the inset of Fig. 1(a), we show a quasiperiodic lattice sample in solid circles, as well as the seed structure in red solid lines. Previous studies showed that such a quasiperiodic structure can support large photonic band

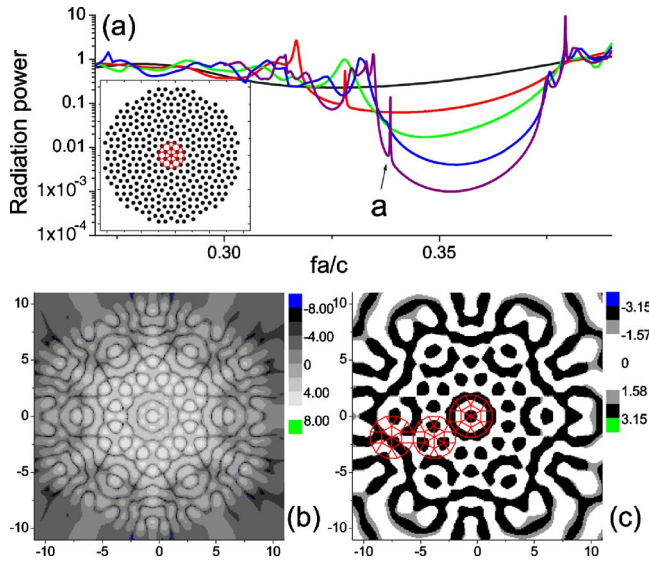


FIG. 1. (Color online) (a) The radiation power spectra for the photonic quasicrystal samples of radii  $R=2a$  (black),  $4a$  (red),  $6a$  (green),  $8a$  (blue), and  $10a$  (purple). The inset graph shows the sample of  $R=10a$ . (b) and (c) show, respectively, the intensity map,  $\ln|E(\vec{r})|^2$ , and phase map,  $\arg[E(\vec{r})]$ , of the band-edge state marked as “a” in (a) for the sample of  $R=10a$ .

gaps.<sup>7,8</sup> Here, we consider the  $s$ -polarized waves, which are described by the following wave equation:

$$-\omega^2 \epsilon(\vec{r}) E(\vec{r}) = c^2 \nabla^2 E(\vec{r}), \quad (1)$$

where  $\omega$ ,  $\epsilon(\vec{r})$ , and  $E(\vec{r})$  are, respectively, the angular frequency, dielectric constant, and electric field.

Equation (1) is solved by using the MST. The MST is a well-established numerical method and has been generally used to solve systems with hundreds of cylinders in the literature.<sup>8,22</sup> However, in this paper, we have to solve much larger systems with tens of thousands of cylinders. The MST gives rise to a set of linear equations. The operation cost of solving these equations is  $O(N_m^3)$ , while the memory cost is  $O(N_m^2)$ . Here,  $N_m$  is the number of cylinders  $N$  multiplied by  $(2m+1)$ .  $m$  is the cutoff angular momentum quantum number used in the calculations. Thus, the calculations become extremely difficult when the number of cylinders is large. However, the difficulty can be overcome by incorporating the so-called SMCG method into the MST.<sup>23,30</sup> The SMCG method is an efficient algorithm based on the decomposition of strong and weak interactions among cylinders. Here, the strong and weak interactions denote the interactions between near and distant cylinders, respectively. Basically, the idea is to utilize a two-dimensional uniform canonical grid which covers the sample. Every cylinder is associated with its nearest grid point. Then, the weak interactions, which accounts for the majority of the required CPU time and memory, can be calculated by using the grid points. With the successive use of the addition theorem, the weak interactions between two distinct cylinders are calculated indirectly from one cylinder to its associated grid point, then from the grid point to the grid point associated with the other cylinder, and finally

from the second grid point to the other cylinder. This facilitates the use of fast Fourier transform, which reduces the operation cost from  $O(N_m^3)$  to  $O(N_m \log N_m)$ .<sup>23,30</sup> In our calculations, we have used an iterative method called the generalized minimal residue (GMRES) method<sup>31</sup> to solve the coupled linear equations given by MST. The GMRES method is very robust and accurate even for dense matrices, and it reduces the memory cost from  $O(N_m^2)$  to  $O(N_m)$ . We have also checked the convergence of our results by increasing  $m$  to 6 and reducing the normwise backward error in GMRES to  $10^{-6}$ . After parallelization, we can solve large systems with tens of thousands of cylinders in a PC cluster.<sup>23</sup>

### III. RESULTS AND DISCUSSIONS

Firstly, we calculate the radiation power spectrum of the photonic quasicrystal. The radiation power is obtained by placing a line source of frequency  $f$  inside a circular sample with radius  $R$  and integrating the output energy flux. The position of the source is deliberately placed beside the center of the sample such that states of any angular momentum quantum number can be excited. The dielectric constant and radii of the dielectric cylinders in the photonic quasicrystal are taken as 4 and  $0.4a$ , respectively. Here,  $a$  is the distance between two nearest cylinders. In Fig. 1(a), we plot the radiation power spectra near the first major band gap of the photonic quasicrystal for small samples of radii  $R=2a$  (black),  $4a$  (red),  $6a$  (green),  $8a$  (blue) and  $10a$  (purple), respectively. When the sample radius is gradually increased, we see that the radiation power in the band gap is reduced exponentially, indicating a quite robust band gap. We also notice that the frequency of the lower band-edge state is shifted toward the band gap with increased sample size, but in an abrupt and irregular way. Since the band-edge state in periodic systems is always shifted smoothly when the sample size is increased, this phenomenon indicates a fundamental difference between quasiperiodic and periodic systems at band edges.

To understand the origin of this phenomenon, we investigate the wave function of these band-edge states. The wave function  $E(\vec{r})$  can be characterized by its intensity map  $|E(\vec{r})|^2$ , as well as its phase map, i.e.,  $\arg[E(\vec{r})] \in (-\pi, \pi)$ . In Figs. 1(b) and 1(c), we plot, respectively, the intensity map and the phase map for the band-edge state in a sample of  $R=10a$ , marked as “a” in Fig. 1(a). The intensity map is plotted in a log scale such that a local resonance of diameter  $d_{res} \approx 16a$  is clearly shown. The local resonance is induced by the local environment within the sample. The phase map exhibits a distinct phase pattern composed of alternating regions with a phase difference  $\pi$ , similar to that of a standing wave. The structure of the phase pattern can also be used to identify the local resonance. In Fig. 1(c), it is interesting to point out that the local phase patterns within the seed structures at different locations can be very different from each other, as is clearly shown in the three seed structures marked by red lines. This implies that the size of the local resonance can be larger than that of the seed structure, which has a diameter of  $d_{seed}=3.8a$ . The sudden appearance of this local resonance when sample radius  $R \geq 10a$  explains the abrupt

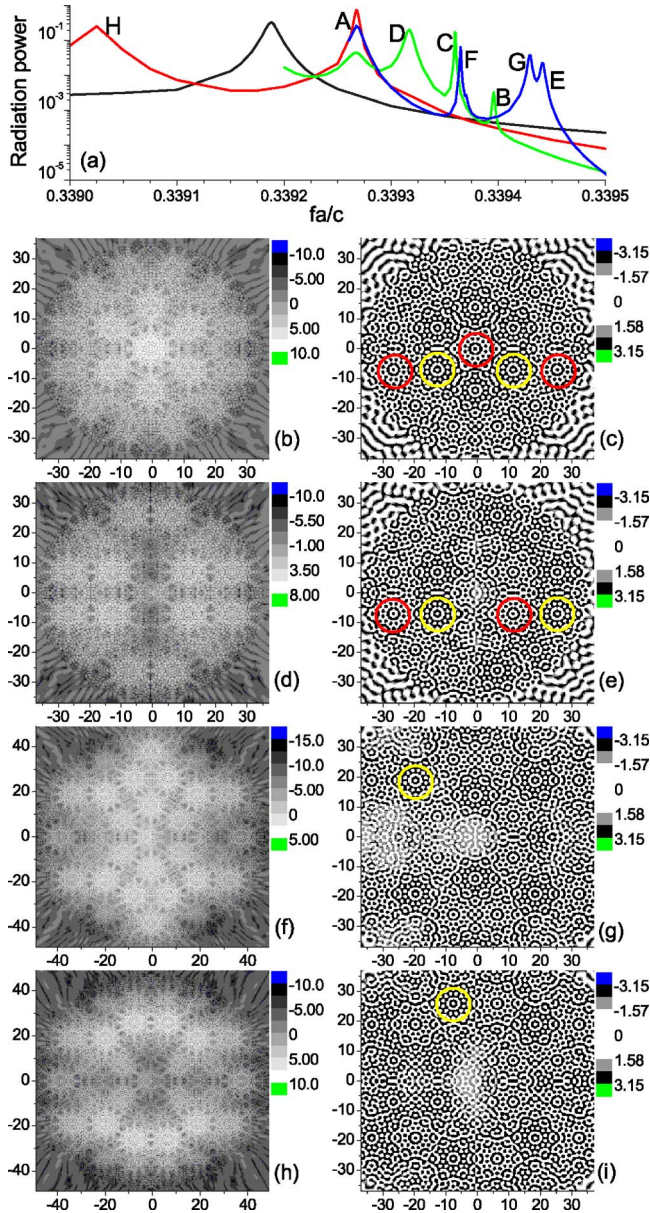


FIG. 2. (Color online) (a) The radiation power spectra for larger photonic quasicrystal samples of radii  $R=24a$  (black),  $36a$  (red),  $48a$  (green), and  $60a$  (blue) near the band edge. (b), (d), (f), and (h) show, respectively, the intensity maps,  $\ln|E(\vec{r})|^2$ , of the states marked as “A,” “H,” “B,” and “C” in (a). (c), (e), (g), and (i) show, respectively, the phase maps,  $\arg[E(\vec{r})]$ , of the states marked as “A,” “H,” “B,” and “C” in (a).

and irregular shift of the band-edge state in Fig. 1(a).

When the sample size is further increased, however, the size of the local resonances does not increase with the sample size. Here, we plot in Fig. 2(a) the band-edge spectra of some large-sized photonic quasicrystal samples of radii  $R=24a$  (black),  $36a$  (red),  $48a$  (green), and  $60a$  (blue). There are 12187 cylinders in the sample of  $R=60a$ . In Figs. 2(b) and 2(c), we plot, respectively, the intensity map and phase map of the band-edge state in a sample of  $R=36a$ , which is marked as “A” in Fig. 2(a). The symmetry of this state obviously coincides with the quasicrystalline structure. In the

phase map, we have observed many repeated local phase patterns as those marked by red and yellow circles in Fig. 2(c). These local patterns are the same as the one shown in Fig. 1(c), apart from a constant phase difference. The local phase patterns marked by the red circles only have a difference of  $\pi$  from those marked by the yellow circles. Their structures coincide with the phase map shown in Fig. 1(c). In Figs. 2(d) and 2(e), we plot, respectively, the intensity map and phase map of the second state from the band edge, which is marked as “H” in Fig. 2(a). This state has a reduced twofold symmetry. From the local phase patterns marked by the red and yellow circles in Fig. 2(e), we can see that it is actually antisymmetric. According to Conway’s theorem, when the sample size is increased, any local environment will always repeat itself.<sup>32</sup> For states A and H, we have observed that more local resonances are induced in the increased part of the sample, while the already existing local resonances are not changed. Both states A and H shift continuously toward the band gap when the sample size is increased.

However, when the sample size is increased to  $R=48a$ , we have observed the sudden emergence of two new states, which are marked as “B” and “C” in Fig. 2(a). The previous band-edge state in the sample of  $R=36a$  has now shifted to “D” in Fig. 2(a). In Figs. 2(f) and 2(g), we show, respectively, the corresponding intensity map and phase map of state B. Obviously, this new band-edge state has a twofold symmetry like state H. However, its intensity map is very different from that of H. To the best of our knowledge, band-edge states with reduced symmetry have not been reported before. In the previous studies on lasing<sup>17</sup> and surface wave functions<sup>16</sup> in quasicrystalline structures, only symmetric band-edge states have been observed. This case shows that band-edge states with reduced symmetry is possible in quasicrystalline systems when the sample size is sufficiently large. In Fig. 2(g), there are still many local phase patterns with the same structure as that in Figs. 2(c) and 2(e). However, many of them exhibit a phase difference of  $\pi$  from those at the same position in Figs. 2(c) and 2(e), as indicated by the yellow circle. In fact, we have checked that the phase pattern in Fig. 2(g) is different from that of any state near the band edge in the smaller sample of  $R=36a$ . This confirms that it is a new state. In Figs. 2(h) and 2(i), we plot, respectively, the intensity map and phase map of state C, which also exhibits a twofold symmetry. The local phase pattern marked by the yellow circle shows a phase difference of  $\pi$  from those at the same position in Figs. 2(c), 2(e), and 2(g). State C is also confirmed to be a new state that emerges in the sample of  $R=48a$ .

When the sample size is further increased to  $R=60a$ , we find that state B disappears, but state C remains and is only slightly shifted to “F” in Fig. 2(a). A new state with a twofold symmetry emerges near the band edge, as marked by “G.” The original band-edge state in the smaller sample of  $R=36a$  is further shifted from D to “E” and becomes the band-edge state again.

The above example shows the complicated situation near the band edges in photonic quasicrystals. Briefly speaking, the band-edge states in photonic quasicrystals are composed of many local resonances whose size could exceed that of the

seed structure. However, when the sample is further increased to a sufficiently large size, new states with reduced symmetry can emerge at the band edge. It is undoubted that the quasiperiodic long-range order has played a key role in generating these new states. The new states observed here are different from the previously observed states emerging in the gaps of phononic quasicrystals, which are induced by the formation of new local resonances and exhibit the same symmetry as the quasiperiodic structure.<sup>23</sup> The observed new states here do not change the local resonances, but seem to support a new kind of coupling among themselves. They could be either sensitive (e.g., state B) or nonsensitive (e.g., state C) to the further increase of sample size.

Here, we have shown that the appearance of new states at the band edge is caused by the couplings of local resonances induced by the local environment in quasiperiodic structures. In a recent paper by Yannopapas *et al.*, it was shown that new states near the band edge of an inverted opal could also be produced by introducing stacking faults, which are a common type of defect, into the inverted opal.<sup>33</sup> A periodic arrangement of the stacking faults can give rise to a narrow band immediately above the lower edge of the original frequency gap. Large transmittance is found for this narrow band due to the periodic coupling of local resonances created at the stacking faults. However, when the stacking faults are arranged randomly, the transmittance becomes very small, negligible for practical purposes. In our work, the local resonances are quasiperiodically arranged inside the sample. Thus, the new band-edge states we have found are intermediate between those created by the periodic stacking faults and those created by random stacking fault in Ref. 33.

The existence of states with reduced symmetries at the band edge might have some useful implications. For example, in Kerr nonlinear photonic crystals, it is known that gap solitons can be excited near the band edge.<sup>34,35</sup> The gap solitons have the same symmetry as that of the band-edge state. Thus, one could expect a gap soliton with reduced symmetry to appear near the band edge when the cylinders are made of materials with Kerr nonlinearity. In Fig. 2(a), we have also noticed that the new states emerging at the band edge often exhibit quite narrow linewidths. A narrower linewidth in spectrum indicates a longer photon lifetime and a higher quality factor. In the previous studies of optical states near band edges, it has been found that the threshold gain is inversely proportional to a photon lifetime, implying that the long photon lifetime is advantageous for achieving low-threshold band-edge lasing action.<sup>28,29</sup> Thus, these new states observed here might be good candidates for low-threshold lasing applications. Because of the reduced symmetry, the light emitted by such states will also be less isotropic.

We have shown the intensity maps of states at the band edge in Fig. 2. Their intensity distributions could be further studied by using the method of the multifractal analysis.<sup>36,37</sup> In the multifractal analysis, the singularity spectrum  $f(\alpha)$  characterizes the scaling properties of the multifractal, where

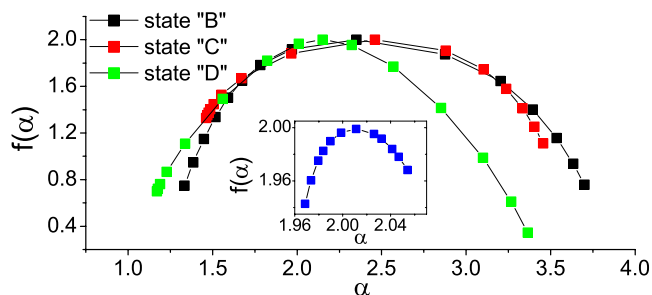


FIG. 3. (Color online) The singularity spectra  $f(\alpha)$  for the states “B,” “C,” and “D” in the photonic quasicrystals of  $R=48a$ . The inset shows  $f(\alpha)$  for the band-edge state in a triangular photonic crystal of  $R=48a$ , which is composed of the same cylinders as those in the photonic quasicrystal.

$\alpha$  characterizes the type of singularities and  $f(\alpha)$  the fractal dimension of the set on which singularities of this type are defined. In Fig. 3, we show the calculated  $f(\alpha)$  for the states marked as B, C, and D in Fig. 2(a), which exist in the sample of  $R=48a$ . For comparison, the  $f(\alpha)$  for the first band-edge state in a triangular photonic crystal sample of the same sample size and cylinders is also shown in the inset graph. The calculations are based on the parametric representations of  $f(q)$  and  $\alpha(q)$  with the same range of moment  $q$  from  $-3$  to  $4$ .<sup>37</sup> It is obvious that  $f(\alpha)$  and  $\alpha$  for the states in the photonic quasicrystal span a much wider range than those in the photonic crystal. This indicates that the fluctuations of the wave functions at band edges in photonic quasicrystals are much larger than those in photonic crystals. We also notice that states B and C exhibit a wider range of  $\alpha$  than state D. This indicates that fluctuations of new states are even larger than those of original band-edge states.

#### IV. CONCLUSIONS

In conclusion, we have studied the nature of band-edge states in large-sized photonic quasicrystals. We have observed the abrupt and irregular evolution of band-edge states as the sample size is increased. The wave functions of the band-edge states exhibit repeated local resonances, which are induced by the repeated clusters in the quasiperiodic structure. New states with reduced symmetry can occur at the band edge in a sufficiently large sample. A strong multifractal behavior and large fluctuations in wave functions are also observed. Our findings unveil some unique properties of the band-edge states in quasiperiodic systems, which are of scientific interests and could be important in applications that utilize these states such as lasing and certain nonlinear optical effects.

#### ACKNOWLEDGMENT

This work was supported by Hong Kong RGC Grant No. CityU 1/02C.

- <sup>1</sup>M. Kohmoto, B. Sutherland, and K. Iguchi, *Phys. Rev. Lett.* **58**, 2436 (1987).
- <sup>2</sup>W. Gellermann, M. Kohmoto, B. Sutherland, and P. C. Taylor, *Phys. Rev. Lett.* **72**, 633 (1994).
- <sup>3</sup>M. A. Kaliteevski, V. V. Nikolaev, R. A. Abram, and S. Brand, *Opt. Spectrosc.* **91**, 109 (2001).
- <sup>4</sup>L. DalNegro, C. J. Oton, Z. Gaburro, L. Pavesi, P. Johnson, A. Legendijk, R. Righini, M. Colocci, and D. S. Wiersma, *Phys. Rev. Lett.* **90**, 055501 (2003).
- <sup>5</sup>Y. S. Chan, C. T. Chan, and Z. Y. Liu, *Phys. Rev. Lett.* **80**, 956 (1998).
- <sup>6</sup>M. A. Kaliteevski, S. Brand, R. A. Abram, T. F. Krauss, R. DeLa Rue, and P. Millar, *Nanotechnology* **11**, 274 (2000).
- <sup>7</sup>M. E. Zoorob, M. D. B. Charlton, G. J. Parker, J. J. Baumberg, and M. C. Netti, *Nature (London)* **404**, 740 (2000).
- <sup>8</sup>X. Zhang, Z. Q. Zhang, and C. T. Chan, *Phys. Rev. B* **63**, 081105(R) (2001).
- <sup>9</sup>W. Man, M. Megens, P. J. Steinhardt, and P. M. Chaikin, *Nature (London)* **436**, 993 (2005).
- <sup>10</sup>B. Freedman, G. Bartal, M. Segev, R. Lifshitz, D. N. Christodoulides, and J. W. Fleischer, *Nature (London)* **440**, 1166 (2006).
- <sup>11</sup>C. Jin, B. Cheng, B. Man, Z. Li, D. Zhang, S. Ban, and B. Sun, *Appl. Phys. Lett.* **75**, 1848 (1999).
- <sup>12</sup>M. Bayindir, E. Cubukcu, I. Bulu, and E. Ozbay, *Phys. Rev. B* **63**, 161104(R) (2001).
- <sup>13</sup>K. Nozaki and T. Baba, *Appl. Phys. Lett.* **84**, 4875 (2004).
- <sup>14</sup>J. Romero-Vivas, D. N. Chigrin, A. V. Lavrinenko, and C. M. Sotomayor Torres, *Opt. Express* **13**, 826 (2005).
- <sup>15</sup>Z. Feng, X. Zhang, Y. Wang, Z.-Y. Li, B. Cheng, and D. Z. Zhang, *Phys. Rev. Lett.* **94**, 247402 (2005).
- <sup>16</sup>M. Torres, J. P. Adrados, J. L. Aragón, P. Cobo, and S. Tehuacanero, *Phys. Rev. Lett.* **90**, 114501 (2003).
- <sup>17</sup>M. Notomi, H. Suzuki, T. Tamamura, and K. Edagawa, *Phys. Rev. Lett.* **92**, 123906 (2004).
- <sup>18</sup>S.-N. Zhu, Y.-Y. Zhu, and N.-B. Ming, *Science* **278**, 843 (1997).
- <sup>19</sup>R. T. Brattfalean, A. C. Peacock, N. G. R. Broderick, K. Gallo, and L. Ruth, *Opt. Lett.* **30**, 424 (2005).
- <sup>20</sup>B. Ma, T. Wang, Y. Sheng, P. Ni, Y. Wang, B. Cheng, and D. Zhang, *Appl. Phys. Lett.* **87**, 251103 (2005).
- <sup>21</sup>R. Lifshitz, A. Arie, and A. Bahabad, *Phys. Rev. Lett.* **95**, 133901 (2005).
- <sup>22</sup>A. DellaVilla, S. Enoch, G. Tayeb, V. Pierro, V. Galdi, and F. Capolino, *Phys. Rev. Lett.* **94**, 183903 (2005).
- <sup>23</sup>Y. Lai, Z. Q. Zhang, C. H. Chan, and L. Tsang, *Phys. Rev. B* **74**, 054305 (2006).
- <sup>24</sup>E. Rotenberg, W. Theis, K. Horn, and P. Gille, *Nature (London)* **406**, 602 (2000).
- <sup>25</sup>S. Noda, M. Yokoyama, M. Imada, A. Chutinan, and M. Mochizuki, *Science* **293**, 1123 (2001).
- <sup>26</sup>Y. Dumeige, I. Sagnes, P. Monnier, P. Vidakovic, I. Abram, C. Meriadec, and A. Levenson, *Phys. Rev. Lett.* **89**, 043901 (2002).
- <sup>27</sup>T. Quang, M. Woldeyohannes, S. John, and G. S. Agarwal, *Phys. Rev. Lett.* **79**, 5238 (1997).
- <sup>28</sup>H.-Y. Ryu, M. Notomi, and Y.-H. Lee, *Phys. Rev. B* **68**, 045209 (2003).
- <sup>29</sup>S. Nojima, *Appl. Phys. Lett.* **79**, 1959 (2001).
- <sup>30</sup>C. H. Chan and L. Tsang, *Microwave Opt. Technol. Lett.* **8**, 114 (1995).
- <sup>31</sup>S. Yousef, *Iterative Methods for Sparse Linear Systems* (PWS, Boston, 1996).
- <sup>32</sup>H. Tsunetsugu, T. Fujiwara, K. Ueda, and T. Tokihiro, *Phys. Rev. B* **43**, 8879 (1991).
- <sup>33</sup>V. Yannopapas, N. Stefanou, and A. Modinos, *Phys. Rev. Lett.* **86**, 4811 (2001).
- <sup>34</sup>S. John and N. Akozbek, *Phys. Rev. Lett.* **71**, 1168 (1993).
- <sup>35</sup>P. Xie and Z.-Q. Zhang, *Phys. Rev. E* **69**, 036601 (2004).
- <sup>36</sup>T. Fujiwara, M. Kohmoto, and T. Tokihiro, *Phys. Rev. B* **40**, 7413 (1989).
- <sup>37</sup>M. Schreiber and H. Grussbach, *Phys. Rev. Lett.* **67**, 607 (1991).